Desalination and Water Treatment
www.deswater.com
doi: 10.5004/dwt.2023.30067

312 (2023) 247–257
November

Adsorption kinetic, equilibrium and thermodynamic studies for the removal of Acid Blue 25 from wastewater by using modified sugarcane bagasse

Hadia Sarwar[a], Noureddine Elboughdiri[b,c], Shagufta Zafar[a,*], Muhammad Imran Khan[d,*], Abdallah Shanableh[d], Jannat Suleman[e], Suryyia Manzoor[f], Ammar Mahjoubi[g], Sami Barkaoui[h], Adnene Midouni[i]

[a]*Department of Chemistry, The Government Sadiq College Women University, Bahawalpur 63000, Pakistan, emails: shg_zf@gscwu.edu.pk (S. Zafar), alia82bwp@gmail.com (H. Sarwar)*
[b]*Chemical Engineering Department, College of Engineering, University of Ha'il, P.O. Box: 2440, Ha'il 81441, Saudi Arabia, email: n.elboughdiri@uoh.edu.sa*
[c]*Chemical Engineering Process Department, National School of Engineering Gabes, University of Gabes, Gabes 6011, Tunisia, email: ghilaninouri@yahoo.fr*
[d]*Research Institute of Sciences and Engineering (RISE), University of Sharjah, Sharjah 27272, United Arab Emirates, email: raoimranishaq@gmail.com (M.I. Khan), Shanableh@sharjah.ac.ae (A. Shanableh)*
[e]*Department of Chemistry, The Women University Multan, Multan 60000, Pakistan, email: jannatchuhan1234@gmail.com*
[f]*Institute of Chemical Sciences, Bahauddin Zakariya University, Multan 60800, Pakistan, email: suryyia.manzoor@bzu.edu.pk*
[g]*Laboratory of "Biodiversity, Molecules and Applications", LR22ES02, Higher Institute of Applied Biology of Medenine,4119 Medenine, University of Gabes, Tunisia, email: mahjoubiammar@yahoo.fr*
[h]*Laboratoire Matériaux Traitement et Analyse INRAP, Technopôle Sidi-Thabet, Tunis 2020, Tunisia, email: samibarkaoui501@gmail.com*
[i]*Useful Materials Valorization Laboratory, National Centre of Research in Materials Science, Technologic Park of Borj Cedria, B.P. 73, 8027, Soliman, Tunisia, email: adnenemidouni@gmail.com*

Received 22 August 2023; Accepted 5 October 2023

ABSTRACT

In this work, batch adsorption of Acid Blue 25 from wastewater onto sugarcane bagasse (SCB) at room temperate was illustrated. The SCB was characterized in term of morphology, Fourier-transform infrared spectroscopy and X-ray diffraction tests. The percentage removal of Acid Blue 25 was increased with contact time, adsorbent (SCB) mass, and temperature while declined with initial concentration of dye in solution and pH. Experimental data of Acid Blue 25 adsorption was subjected to linear and non-linear pseudo-first-order and pseudo-second-order kinetic models. Results showed that Acid Blue 25 adsorption onto SCB from wastewater fitted to linear and non-linear pseudo-second-order model. Two, three and four parameters non-linear adsorption isotherms models were used to demonstrate adsorption of Acid Blue 25 onto SCB. Attained results showed that adsorption of Acid Blue 25 followed non-linear Langmuir isotherm model. Results of adsorption thermodynamics study represented that adsorption of Acid Blue 25 from wastewater onto SCB was an endothermic because the value of change in enthalpy was positive ($\Delta H°$ = 7.455 kJ/mol). In addition, adsorption of Acid Blue 25 onto SCB was feasible and spontaneous process. In addition, the regeneration of adsorbent is also reported.

Keywords: Sugarcane bagasse; Adsorption; Endothermic process; Non-linear pseudo-second-order model; Acid Blue 25; Non-linear Langmuir isotherm

* Corresponding authors.

1. Introduction

Water is a crucial natural resource on earth, but it can become contaminated through the introduction of various pollutants. When water is no longer suitable for its intended purposes, it is considered polluted. Identifying the types of pollutants present in the water is an important first step in addressing this issue. Water contamination can occur due to the intake of minerals, organic compounds, or solid waste into water bodies. These chemicals are introduced through industrial, commercial, residential, healthcare, agricultural, and other sources [1–4]. Many industrial wastewaters contain organic contaminants, with dyestuffs from industries like textiles, leather, and paper posing significant challenges [5,6]. Dyes are also used in the plastics, pharmaceuticals, food, and cosmetics industries [7]. Some dyes have adverse effects on the immune system, leading to strong reactions when inhaled, such as coughing, sneezing, watery eyes, and asthma symptoms [8]. The contamination of water resources with dyes is of great concern for various problems [9]. Addressing these issues requires the treatment of polluted water.

Various methods have been employed to decolorize and remove dyestuffs from wastewater, including coagulation, electro-oxidation, adsorption, advanced oxidation processes, flocculation, biological degradation, and membrane processes [10,11]. Among these methods, adsorption is particularly noteworthy for its effectiveness, versatility, reliability, simplicity, and wide range of available adsorbents [12–16]. It is also advantageous due to its affordability, ability for adsorbent regeneration, applicability to various adsorbates, absence of pre-treatment requirements, and lack of long-term toxic residues [9,11,17].

Adsorbents like banana pith [18], date leaves [7], rice husk [19], plant leaves powder [20–23], activated carbon [24] and orange peels [25], are excellent adsorbents to remove dyes from wastewater [26]. Among these adsorbents, sugarcane bagasse (SCB) stands out as a low-cost and eco-friendly biosorbent. SCB primarily consists of lignin, cellulose, and hemicellulose, making it an excellent precursor for water purification as an adsorbent. In order to enhance its adsorption efficiency, modifications can be made to the SCB [27]. Globally, approximately 100 million tons of SCB, an agricultural waste by-product, is generated each year by the sugarcane industry. Currently, a significant portion of SCB is burned for energy production, which not only harms the environment but also wastes this valuable bioresource [28]. SCB is abundantly available, affordable, and possesses a polymeric structure consisting of 50% cellulose, 25% lignin, and 25% hemicellulose. Therefore, utilizing this industrial waste as a low-cost adsorbent could yield a dual benefit by reducing environmental pollution [29].

In this work, the removal of dyes from an aqueous solution was investigated in batch mode, with a focus on analyzing the impact of various parameters such as adsorbent dosage, temperature, contact time, pH and initial dye concentration. Different kinetics models were applied to the experimental data, allowing for the interpretation and comparison of kinetic parameters. Experimental data of Acid Blue 25 adsorption onto SCB was also subjected to several linear and non-linear isotherm models. Furthermore, thermodynamic parameters, including changes in Gibbs' free energy, entropy, and enthalpy, were determined for the adsorption of Acid Blue 25 onto SCB at different temperatures. The regeneration of adsorbent was also studied.

2. Experimental work

2.1. Adsorbent

SCB was obtained from a local sugar mill in Bahawalpur, Pakistan. It was subjected to a series of preparation steps to ensure its suitability as an adsorbent. First, the SCB was thoroughly dried, washed, and cleaned. Distilled water was used to rinse it and remove any impurities. The dried SCB was then divided into smaller pieces and placed in a hot air oven at 80°C for 24 h to ensure complete drying. After drying, the pieces were grinded into a fine powder using a mixer grinder. The resulting powder was sieved to ensure uniform particle size distribution, retaining only the useful particles. To enhance its adsorption capacity, the SCB powder was treated with a 0.1 M NaOH solution. Finally, the treated SCB powder was stored in an airtight container for later use.

2.2. Adsorbate

In this research, Acid Blue 25 dye was used as the adsorbate. A stock solution of Acid Blue 25 dye with a concentration of 1,000 ppm was prepared in a 500 mL of distilled water. Further dilutions of the stock solution were made as per the experimental requirements. The chemical structure of Acid Blue 25 dye is given in Fig. 1.

2.3. Adsorption test

In this study, batch adsorption experiments were conducted to investigate the adsorption of Acid Blue 25 onto SCB, following established procedures [30–37]. Initially, the measured amount of SCB was shaked at a fixed speed of 180 rpm into known volume of dye solution and concentration of Acid Blue 25 solutions at room temperature. The concentration of Acid Blue 25 was measured using UV/VIS spectrophotometer (UV-2550, SHIMADZU, Kyoto, Japan) at wavelength of 550 nm.

2.4. Instrumentations

Morphology of SCB was investigated by utilizing scanning electron microscopy (SEM). Fourier-transform infrared

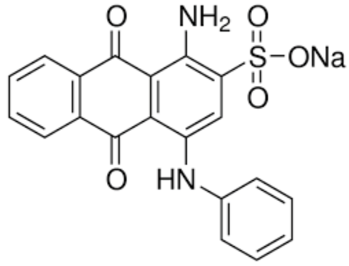

Fig. 1. Chemical structure of Acid Blue 25.

(FTIR) spectroscopy and X-ray diffraction (XRD) tests of SCB were also conducted. Surface area of SCB was determined by Brunauer–Emmett–Teller (BET).

3. Results and discussion

3.1. XRD test

The XRD pattern of NaOH treated SCB was recorded to study the changes in the crystallinity of fibers during the course of modification. The crystalline nature of cellulose was revealed from major peaks at 15.85 and 22.15 in XRD patterns of NaOH treated SCB as shown in Fig. 2 [38].

3.2. FTIR test

Herein, we carried out FTIR analysis of SCB and attained results are given in Fig. 3. The peak at 2,920 cm^{-1} was associated to the asymmetric and symmetric stretching vibration of methylene (–CH_2) group [39,40]. The bold absorption band of carboxylic acid group, C–OH stretch at 1,030 cm^{-1} was existed in cellulose. The broad band at 3,370 cm^{-1} was attributed to the existence of hydroxyl group, O–H in cellulose, hemicellulose, and pectin [39–41]. The peaks at 1,728.25 and 1,603.76 cm^{-1} represented stretching vibrations of carbonyl group (C=O) and alkene group (C=C).

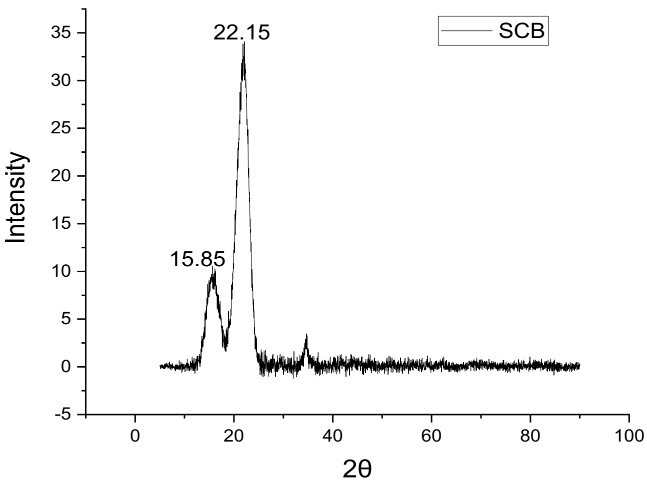

Fig. 2. X-ray diffraction pattern of NaOH-treated SCB.

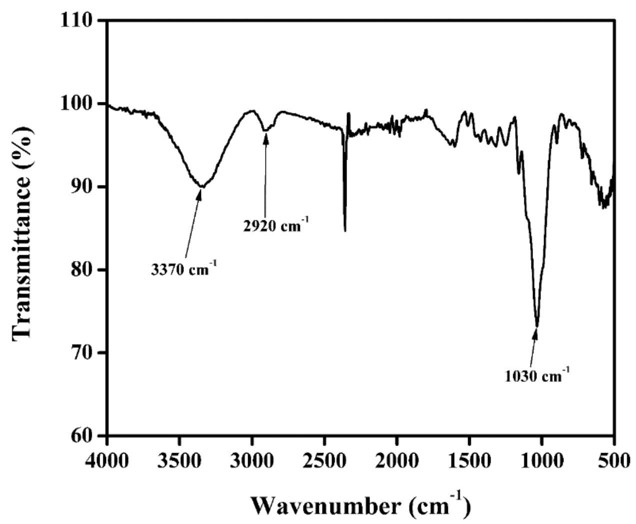

Fig. 3. Fourier-transform infrared spectrum of SCB.

3.3. SEM analysis of SCB

Morphology of SCB was illustrated by using SEM. Adsorptions of dyes are also dependent on structure of adsorbents. Fig. 4 represents the SEM micrograph of SCB. It can be seen that SCB has irregular and rough morphologies. In addition, pores or holes were also noted on SEM micrograph of SCB. From here, it can be concluded that observed structure of SCB is useful for Acid Blue 25 adsorption from wastewater.

3.4. BET test

The surface area, pore size, and pore volume of SCB was determined by utilizing BET. The surface area, pore size, and pore volume of SCB were 4.90 m^2/g, 2,417 A and 0.30 cm^3/g, respectively [42]. It showed that SCB exhibited higher pore size and surface area. Pore volume describes saturation of the pore with N_2 at the greatest relative pressure (P/P^0), where P/P^0 = 0.99 [42]. From here, it is expected that SCB could adsorb more Acid Blue 25 dye molecule due to its larger surface area.

3.5. Effect of operating factors on the Acid Blue 25 removal from wastewater

The duration of contact time played a significant role in the efficiency of the adsorption process. The impact of contact time on the adsorption of Acid Blue 25 was investigated at room temperature, while maintaining a constant Acid Blue 25 dye concentration of 30 mg/L and an adsorbent dose of (0.15 g). The obtained results are shown in Fig. 5a. It was observed that the adsorption of acid blue dye onto SCB increased as the contact time increased. After 90 min of contact time, a maximum adsorption of

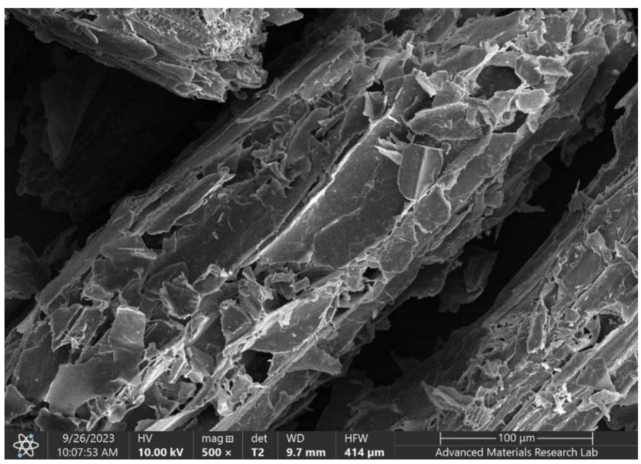

Fig. 4. Scanning electron micrograph of SCB.

approximately 84% was achieved on the surface of SCB. The initial stages of the adsorption process exhibited higher efficiency as there were more vacant active sites [43–45]. However, as time passed, the number of empty sites on SCB decreased, resulting in a decrease in the adsorption rate. Based on these observations, time duration of 90 min was determined as the optimal duration and was used for subsequent experiments. Table 1 provides an interesting comparison of Acid Blue 25 adsorption onto SCB with other adsorbents reported in literature.

Adsorbent mass is a significant factor that is essential to the process of adsorption. The effect of SCB dose on the removal of Acid Blue 25 dye was studied by maintaining all other experimental conditions constant in order to observe the least dose that gives maximum adsorption and obtained results are given in Fig. 5b. The percentage of dye removal was increased with increasing the SCB dosage from 0.01 to 0.3 g. It was removed to a maximum of 80.37% at 0.15 g at room temperature. It was associated to increase in number adsorption sites with the increase in amount of adsorbent as reported in our previous work [46,47]. It showed that the optimized SCB dosage for removing Acid Blue 25 dye was found to be 0.15 g.

Fig. 5c indicates the influence of initial concentration of Acid Blue 25 on the percentage removal of Acid Blue 25 from wastewater at room temperature. It was illustrated by changing initial concentration of dye from 10 to 150 mg/L at room temperature maintaining other factors constant. As shown in Fig. 5c, the percentage removal of Acid Blue 25 was reduced with increase in dye initial concentration. It was attributed to saturation of active sites on the adsorbent surface with increasing concentration of Acid Blue 25 in the dye solution [43,48]. The adsorption capacity was higher

Table 1
Comparison of Acid Blue 25 adsorption onto SCB with other adsorbents reported in the literature

Adsorbents	Removal of Acid Blue 25 (%)	References
Base treated *Shorea dasyphylla* sawdust	98	[53]
Magnetic-SBA-15/CPAA	90	[54]
Magnetic-SBA-15	58	[54]
Cross-linked PAA	69	[54]
Nano-porous functionalized hydroxyapatite	88	[55]
Sugarcane bagasse (SCB)	84	This work

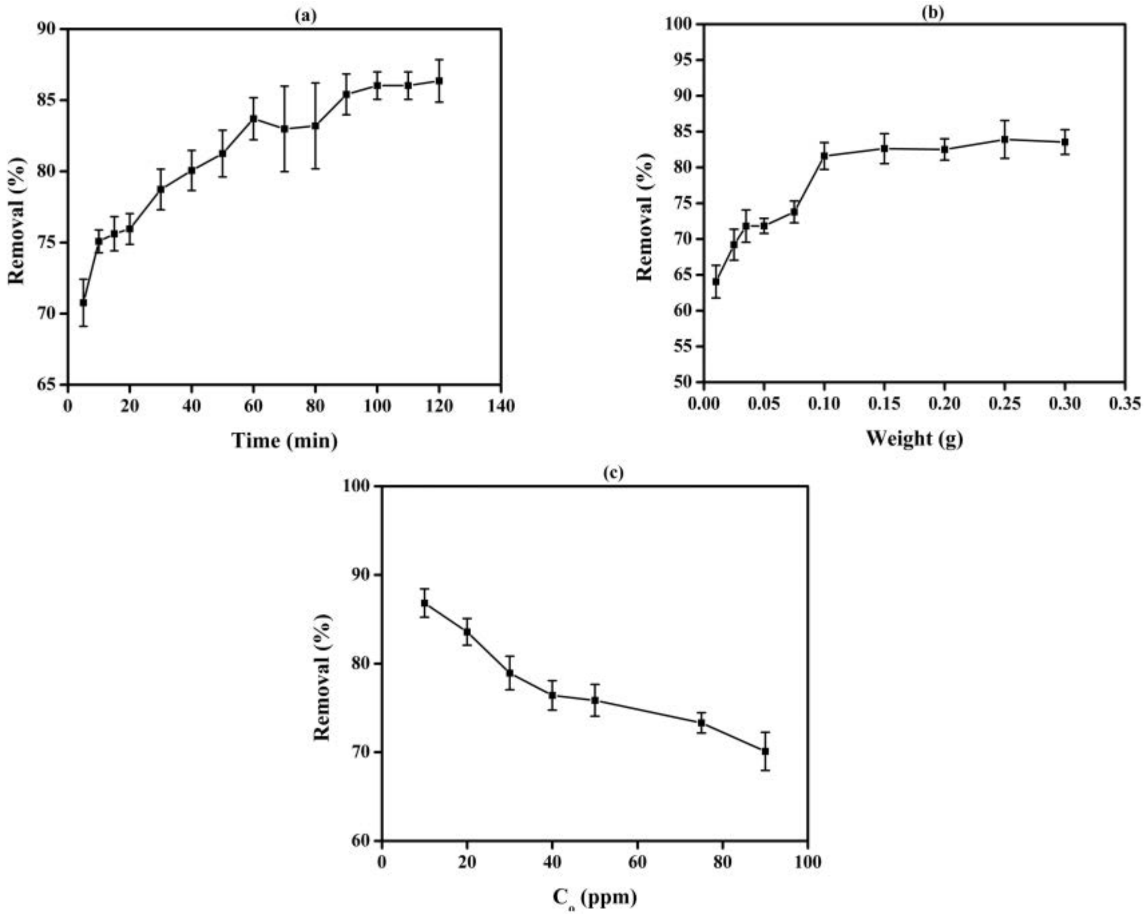

Fig. 5. (a) Effect of time duration, (b) mass of adsorbent (SCB), (c) initial concentration of the Acid Blue 25 dye on the percentage removal from wastewater.

in low concentrations due to the availability of free active sites as reported in our previous work [32,49].

Temperature plays a significant role in the removal of dyes from wastewater. To investigate the effect of temperature on the removal of Acid Blue 25 dye, an optimized weight of 0.15 g of SCB was added to a 30 mL solution containing 30 mg/L of the dye. The temperature was varied from 283 to 328 K, while the mixture was shaken for duration of 90 min. The results of this experiment are presented in Fig. 6a. It was observed that the percentage removal of Acid Blue 25 dye increased from 74% to 82% with an increase in temperature. This indicates that the adsorption of Acid Blue 25 onto SCB was an endothermic process, in agreement with previous studies [50,51].

The pH of medium plays a significant for adsorption of dyes from wastewater. Fig. 6b indicates the influence of pH on the percentage removal of Acid Blue 25 dye from wastewater by using SCB at room temperature. It can be seen that the removal of Acid Blue 25 from wastewater was decreased with increase in pH of medium. At lower pH (pH = 1), the SCB possess higher number of positively charged surfaces which resulted to higher removal of Acid Blue 25 from wastewater. It was associated to the electrostatic for attraction between positively charged SCB surfaces and negatively charged dye molecules. With increase in pH of medium from 2 to 9, the dye removal was declined due to decrease in number of positively charged surfaces and enhancement in number of negatively charged surfaces. It was due electrostatic force of repulsion between SCB and Acid Blue 25 dye molecules in solution. The of zero-point charge pH_{ZPC} of SCB was 4.20 as described [52].

3.6. Adsorption kinetics

3.6.1. Non-linear adsorption kinetics

3.6.1.1. Linear pseudo-first-order model

The linearized form of the Lagergren pseudo-first-order rate equation is represented as [56,57].

$$\log\left(q_e - q_t\right) = \log q_e - \frac{K_1 t}{2.303} \quad (1)$$

where q_e and q_t is the adsorbed amount of dye at equilibrium and time t, respectively and K_1 (min^{-1}) is the rate constant of pseudo-first-order adsorption model. For Acid Blue 25 adsorption on SCB, the plot of log(q_e–q_t) vs. time is denoted in Fig. 7a. Determined values of parameters (K_1 & q_e) are given in Table 2. The value correlation coefficient (R^2 = 0.955) was smaller than unity. In addition, there was a big difference between the values of experimental adsorption capacity ($q_{e,\exp}$) and calculated adsorption capacity values ($q_{e,\text{cal}}$) Table 2. It suggested that the pseudo-first-order model cannot explain the rate process.

3.6.1.2. Linear pseudo-second-order model

The linearized form of pseudo-second-order kinetic model is represented as [57,58]

$$\frac{t}{q_t} = \frac{1}{k_2 q_e^2} + \frac{t}{q_e} \quad (2)$$

where k_2 (g/mg·min) is the rate constant of pseudo-second-order model. Fig. 7b shows graphical representation of pseudo-second-order model. Measured values of its factors are given in Table 2. It can be seen that the experimental adsorption capacity (5.10 mg/g) and calculated

Table 2
Measured linear kinetic parameters for adsorption of Acid Blue 25 onto SCB

Linear kinetic models	Determined factors	
Pseudo-first-order	$q_{e,\exp}$	5.10
	$q_{e,\text{cal}}$	1.048
	K_1	0.030
	R^2	0.955
Pseudo-second-order	q_e	5.20
	k_2	0.069
	R^2	0.999

k_2: g/mg·min; q_e: mg/g; K_1: (min^{-1})

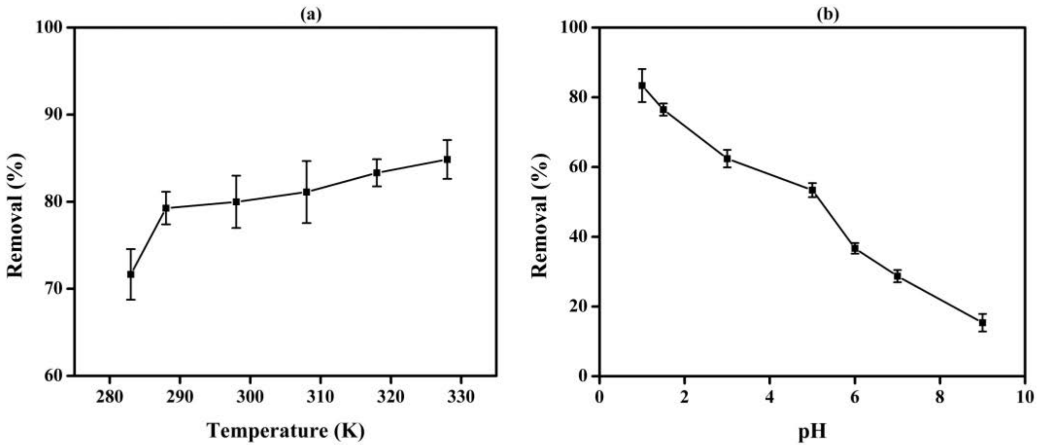

Fig. 6. (a) Effect of temperature and (b) effect of pH on the dye percentage removal from wastewater.

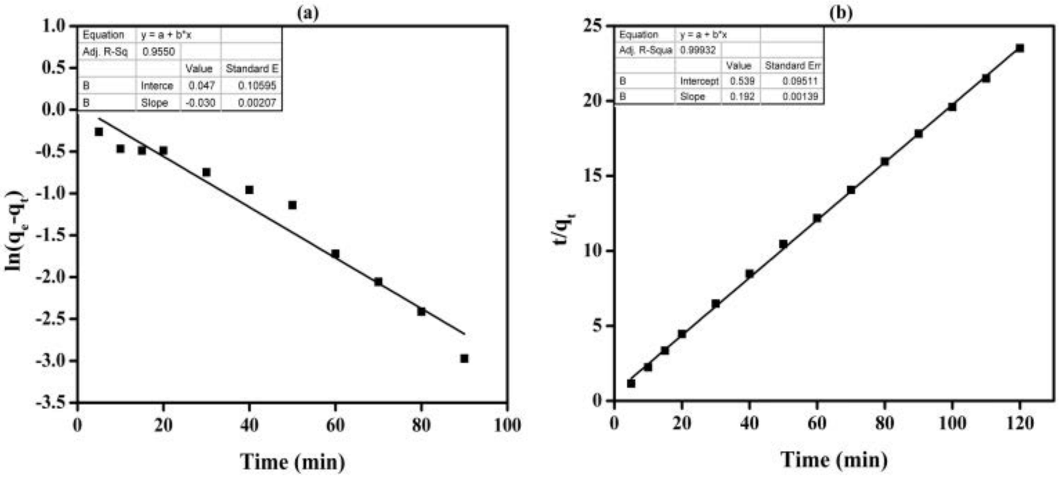

Fig. 7. (a) Linear pseudo-first-order model and (b) linear pseudo-second-order model for Acid Blue 25 adsorption onto SCB from wastewater.

adsorption capacity (5.20 mg/g) values are close to each other (Table 2). Moreover, the value of correlation coefficient (R^2 = 0.999) was close to unity representing that Acid Blue 25 adsorption fitted to pseudo-second-order model.

3.6.2. Non-linear adsorption kinetics

Non-linear pseudo-first-order and pseudo-second-order models were utilized to demonstrate adsorption kinetics for Acid Blue 25 adsorption onto SCB. Herein, IGOR Pro 6.1.2, Wave Metrices software was used to determine the values of adsorption kinetics endowments.

Non-linear pseudo-first-order model is shown as [48,59]:

$$\frac{dQ_t}{dt} = k_1\left(Q_e - Q_t\right) \tag{3}$$

Non-linear pseudo-second-order model is expressed as [48,59]:

$$\frac{dQ_t}{dt} = k_2\left(Q_e - Q_t\right)^2 \tag{4}$$

where Q_e (mg/g) indicates the quantity adsorbed at equilibrium, Q_t represents quantity adsorbed at "t", time, K_1 and k_2 (g/mg·min) indicate pseudo-first-order and pseudo-second-order rate constants, t (min) represents time.

Non-linear pseudo-first-order model is represented as:

$$Q_t = Q_e\left(1 - e^{-kt}\right) \tag{5}$$

Non-linear pseudo-second-order model is denoted as:

$$Q_t = \frac{k_2 Q_e^2 t}{1 + k_2 Q_e t} \tag{6}$$

The graphical representation of non-linear pseudo-first-order and pseudo-second-order kinetics models are shown in Fig. 8. Determined values of experimentally measured constants and theoretical Q_e values are given in Table 3.

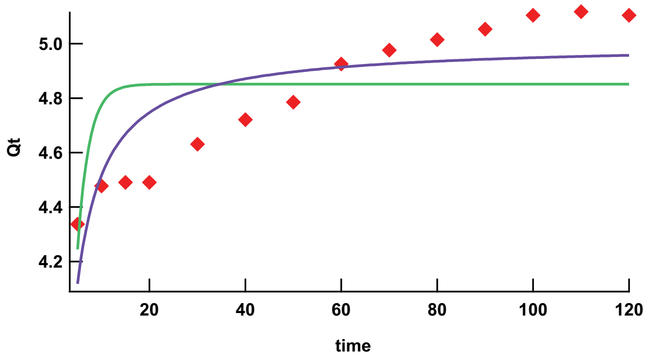

Fig. 8. Non-linear plots of pseudo-first-order and pseudo-second-order kinetics models for of Acid Blue 25 adsorption onto SCB from wastewater.

Table 3
Measured non-linear kinetic parameters for adsorption of Acid Blue 25 on sugarcane bagasse

Non-linear kinetic models	Determined factors	
	q_e	4.851
Pseudo-first-order	K_1	0.415
	χ^2	0.707
	q_e	5.001
Pseudo-second-order	k_2	0.186
	χ^2	0.315

Chi-square test 'χ^2' was utilized to describe which model supported the kinetic equations with best fit.

$$\chi^2 = \sum \frac{\left(Q_e - Q_{e,m}\right)^2}{Q_{e,m}} \tag{7}$$

where Q_e (mg/g) represents equilibrium capacity determined utilizing experimental data and $Q_{e,m}$ (mg/g) represents equilibrium capacity computed through model. The values of 'χ^2' for these kinetic models are given in Table 3. The comparison of model-derived data with experimental data represented that whether the data are similar in this instance 'χ^2' would denote a limited number and vice versa. To measure kinetic constants for pseudo-second-order model is more trustworthy as demonstrated by the attained lower 'χ^2' (non-linear) values.

3.7. Adsorption isotherms

3.7.1. Two parameters non-linear adsorption isotherms

Non-linear Freundlich, Langmuir, Dubinin–Radushkevich (D-R), and Temkin isotherms were used to investigate Acid Blue 25 adsorption on SCB. To perform the non-linear regression analysis, Igor Pro. WaveMatrices 6.2.1 was employed [46,60]. To determine the most suitable model for describing the adsorption of Acid Blue 25 onto SCB, a statistical tool called the non-linear chi-square (χ^2) analysis was applied.

Non-linear Langmuir isotherm is expressed as [57].

$$q_e = \frac{Q_m k_L C_e}{1 + k_L C_e} \quad (8)$$

where Q_m (mol/g) represents the Langmuir mono-layer adsorption capability, while K_L (L/mol) corresponds to the Langmuir constant. Fig. 9 represents non-linear Langmuir isotherm for Acid Blue 25 adsorption onto SCB from wastewater. The values of its parameters are given in Table 4. It was noted that non-linear Langmuir isotherm model best described the Acid Blue 25 adsorption onto SCB from wastewater as represented by lower chi-square value ($\chi^2 = 2.057$)

Non-linear Freundlich isotherm is shown as [46,57]:

$$q_e = K_f C_e^{1/n} \quad (9)$$

where n and K_f are the parameters associated with the Freundlich isotherm. Fig. 9 illustrates the Freundlich isotherm for the adsorption of Acid Blue 25 onto SCB from wastewater, and the corresponding Freundlich parameters can be found in Freundlich isotherm for Acid Blue 25 adsorption onto SCB from wastewater and attained values of Freundlich endowments are given in Table 4. Non-linear Freundlich isotherm followed Acid Blue 25 adsorption onto SCB as indicated by lower chi-square value ($\chi^2 = 7.556$).

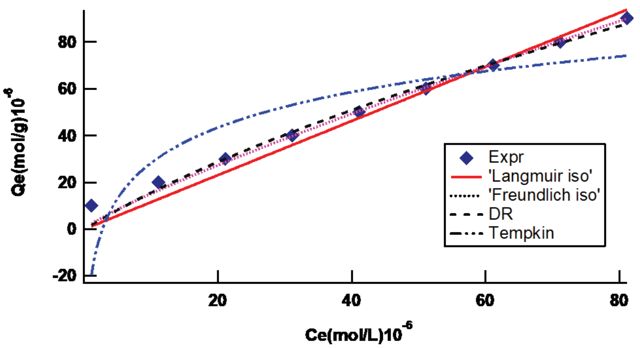

Fig. 9. Non-linear plots of Freundlich, Langmuir, Dubinin–Radushkevich and Temkin isotherms for the adsorption of Acid Blue 25 on SCB from wastewater.

Non-linear Temkin adsorption isotherm is expressed as:

$$q_e = \frac{RT}{b_T} \ln\left(a_T C_e\right) \quad (10)$$

where R (J/mol·K) and T (K) indicate gas constant and absolute temperature, respectively. b_T and a_T are attributed with heat of adsorption and equilibrium binding constant corresponding to highest binding energy, respectively. Non-linear Temkin adsorption isotherm is depicted in Fig. 9. Determined values of b_T and a_T are given in Table 4. The chi-square value represented that non-linear Temkin adsorption isotherm followed experimental data for Acid Blue 25 adsorption onto SCB from wastewater.

Non-linear D-R isotherm is expressed as:

$$q_e = C_m \exp\left(-\beta \varepsilon^2\right) \quad (11)$$

the Polanyi potential "ε" is given as:

$$\varepsilon = RT \ln\left(1 + \frac{1}{C_e}\right) \quad (12)$$

where β shows mean adsorption energy in Eq. (6):

$$E = \frac{1}{\sqrt{2\beta}} \quad (13)$$

Non-linear D-R isotherm for acid blue adsorption onto SCB is shown in Fig. 9. For Acid Blue 25 adsorption onto SCB, the attained value of mean adsorption energy (8.80 kJ/mol) showed that it was chemical adsorption process [33,61].

Table 4
Determined endowments of two parameters non-linear isotherms

Two parameters non-linear adsorption isotherms	Determined factors		
Langmuir isotherm	Q_m	K_L	χ^2
	0.539	2.146	2.057
Freundlich isotherm	K_f	n	χ^2
	0.270	1.176	7.556
Temkin isotherm	b_T	a_T	χ^2
	1.198	3.636	1.814
Dubinin–Radushkevich isotherm	B	Q_m	χ^2
	0.0065	0.0028	9.302
		$E = 8.80$	

Q_m: mg/g; K_L: L/mol; K_f: mol/g; b_T: kJ/mol; a_T: L/mg; β: mol²/J²; C_m: mg/g; E: kJ/mol

3.7.2. Three parameters non-linear adsorption isotherms

Fig. 10 illustrates the application of three-parameter isotherms (Toth, Hill, Redlich–Peterson, and Sips) for Acid Blue 25 adsorption onto SCB from wastewater.

Non-linear Toth isotherm is represented as:

$$Q_e = \frac{k_T C_e}{\left(a_T + C_e\right)^{1/t}} \tag{14}$$

where k_T, T and a_T denote Toth isotherm constants. Fig. 10 shows non-linear Toth isotherm for Acid Blue 25 adsorption onto SCB. The smaller chi-square value (χ^2 = 1.776) indicated that Toth isotherm followed Acid Blue 25 adsorption onto SCB. Measured Toth constants (k_T, a_T and T) are given in Table 5.

Non-linear Hill isotherm is represented as:

$$Q_e = \frac{q_h C_e^{n_h}}{K_H + C_e^{n_h}} \tag{15}$$

where K_H, q_h and n_h are Hill isotherm constants. Non-linear Hill isotherm plot is indicated in Fig. 10. Measured values of its parameters (K_H, n_h, and q_h) are shown in Table 5. Lower value of χ^2 (6.289) represented that experimental data followed Hill isotherm.

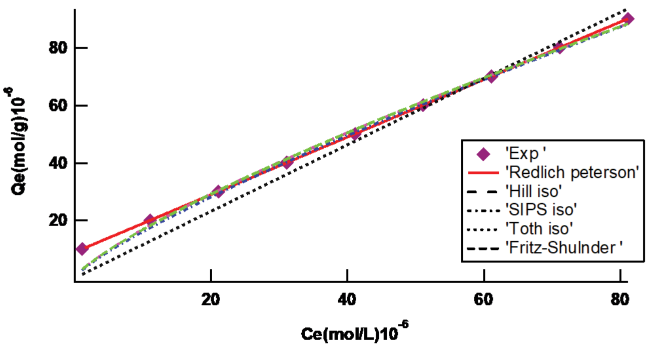

Fig. 10. Non-linear plots of Redlich–Peterson, Hill, Sips, Toth, Fritz–Schlunder for the adsorption of Acid Blue 25 on SCB from wastewater.

Table 5
Determined endowments of three parameters non-linear isotherms

Three parameters non-linear adsorption isotherms	Determined factors			
Redlich–Peterson	K	A	G	χ^2
	0.236	0.276	0.934	1.776
Hill isotherm	q_h	n_h	K_H	χ^2
	0.466	0.791	3.059	6.289
Toth isotherm	k_T	a_T	T	χ^2
	1.494	0.083	0.137	2.012
Sips isotherm	K_s	β_s	a_s	χ^2
	0.171	0.806	–38.13	6.589

K_s: L/g; a_s: L/g; q_h: mg/g; K_H: (mg)^{nh}; k_T: mg/g

Non-linear Redlich–Peterson isotherm is represented as:

$$Q_e = \frac{K_{\text{RP}} C_e}{1 + a_{\text{RP}} C_e^{g}} \tag{16}$$

where K, a and g are the Redlich–Peterson's isotherm parameters. Non-linear Redlich–Peterson isotherm is indicated in Fig. 10. Calculated Redlich–Peterson constants (K, a and g) values are shown in Table 5. Smaller chi-square value (χ^2 = 1.776) indicated that experimental data for Acid Blue 25 followed Redlich–Peterson isotherm.

Non-linear Sips isotherm is expressed as:

$$Q_e = K_s \frac{C_e^{\beta_s}}{1} + a_s C_e^{\beta_s} \tag{17}$$

where K_s and a_s show Sips isotherm model constants whereas β_s indicates Sips isotherm exponent. Non-linear Sips isotherm plot is shown in Fig. 10. Determined values of its parameters are given in Table 5. Results illustrated adsorption of Acid Blue 25 followed Sips isotherm model.

3.7.3. Four parameters non-linear adsorption isotherms

Non-linear Fritz–Schlunder isotherm is expressed as:

$$q_e = \frac{A C_e^{\alpha}}{1 + B C_e^{\beta}} \tag{18}$$

where q_e represents the adsorbed amount at equilibrium (mg/g), C_e is the equilibrium concentration of the adsorbate (mg/L), and A and B are the Fritz–Schlunder parameters. Additionally, α and β are the Fritz–Schlunder equation exponents.

The graphical representation of Fritz–Schlunder isotherm is shown in Fig. 10. Attained results showed that Acid Blue 25 adsorption onto SCB followed Fritz–Schlunder isotherm with lower chi-square value (χ^2 = 6.299).

3.8. Adsorption thermodynamics

We illustrated adsorption thermodynamics of Acid Blue 25 onto SCB by determining the change in Gibb's free energy ($\Delta G°$), enthalpy ($\Delta H°$) and entropy ($\Delta S°$) by using relationship:

$$\ln K_c = \frac{\Delta S°}{R} - \frac{\Delta H°}{RT} \tag{19}$$

$$K_c = \frac{C_a}{C_e} \tag{20}$$

$$\Delta G° = \Delta H° - T\Delta S° \tag{21}$$

where K_c, $\Delta G°$, $\Delta H°$ and $\Delta S°$ are equilibrium constant, change in Gibb's free energy (kJ/mol), enthalpy (kJ/mol) and entropy (J/mol·K), respectively. For Acid Blue 25 adsorption onto SCB, the graph of $1/T$ vs. $\ln K_c$ is shown in Fig. 11. The positive value of entropy ($\Delta S°$ = 0.035 J/mol) indicated the increase in randomness at adsorbate–adsorbent interface during Acid Blue 25 adsorption onto SCB from

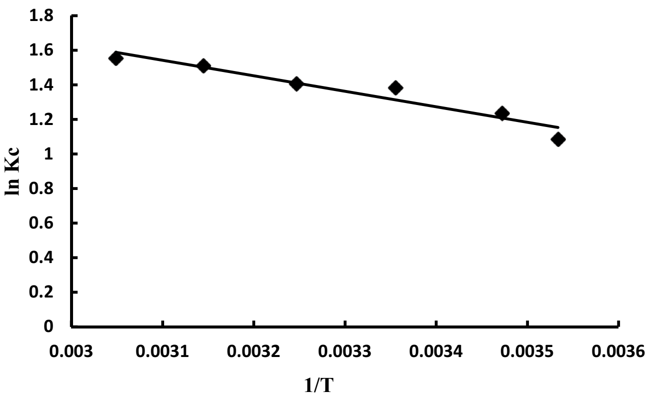

Fig. 11. Plot of 1/*T* vs. ln*k* for adsorption of Acid Blue 25 on sugarcane bagasse.

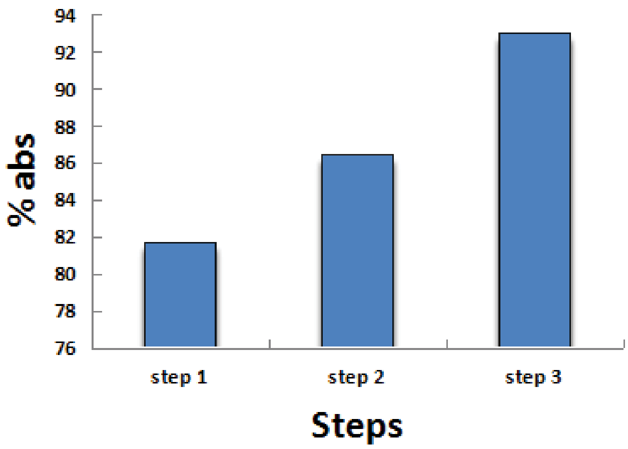

Fig. 12. % adsorption of Acid Blue 25 on sugarcane bagasse in different cycles.

wastewater [62,63]. Likewise, the positive value of enthalpy ($\Delta H°$ = 7.455 kJ/mol) indicated that Acid Blue 25 adsorption onto SCB was endothermic process [59,62]. With the rise in temperature, the decrease in Gibb's free energy from –2.713 to –4.331 kJ/mol shows a decline in the feasibility of adsorption at elevated temperature [51]. In addition, its negative value of Gibb's free energy exhibited that the Acid Blue 25 adsorption onto SCB was spontaneous in nature [62,63].

3.9. Regeneration

To reveal the environmental application of the SCB simultaneous removal of Acid Blue 25 dye was achieved in a tap water sample by a batch process. Tap water was collected from the Department of chemistry, Government Sadiq College Women University, Bahawalpur, Pakistan. A stock solution of dye was prepared in tap water and required concentration was obtained by further dilution. An optimum amount of adsorbent 0.15 g of SCB and 30 mL of Acid Blue 25 dye was taken in culture tube placed on orbital shaker. After this, the initial absorbance of the sample was calculated. It was noted that the adsorption of Acid Blue 25 was 93.25%. These results indicated the good applicability of SCB for dyes removal from water samples. The percentage adsorption of Acid Blue 25 dye is given in Fig. 12.

4. Conclusion

Herein, adsorption of Acid Blue 25 onto SCB from wastewater at room temperature was evaluated. The percentage removal of dye was increased with adsorbent dose, temperature and contact time while declined with dye initial concentration and pH. adsorption kinetics results exhibited that adsorption of Acid Blue 25 onto SCB fitted to linear and non-linear pseudo-second-order kinetics because the value of correlation coefficient (R^2 = 0.999) was close to unity. Adsorption isotherm study results represented that adsorption of Acid Blue 25 fitted to non-linear Langmuir isotherm. In addition, adsorption of Acid Blue 25 was chemical adsorption process. Adsorption thermodynamics investigations represented that this was endothermic and spontaneous process. These results indicated that the SCB has great potential for removal of the Acid Blue 25 dye from the wastewater.

Acknowledgements

The authors are highly thankful to Government Sadiq College Women University (GSCWU), Bahawalpur, Pakistan for financial support.

References

[1] I. Ali, A.A. Basheer, X.Y. Mbianda, A. Burakov, E. Galunin, I. Burakova, E. Mkrtchyan, A. Tkachev, V. Grachev, Graphene based adsorbents for remediation of noxious pollutants from wastewater, Environ. Int., 127 (2019) 160–180.

[2] A.A. Basheer, New generation nano-adsorbents for the removal of emerging contaminants in water, J. Mol. Liq., 261 (2018) 583–593.

[3] I. Ali, Z.A. Alothman, A. Al-Warthan, Sorption, kinetics and thermodynamics studies of atrazine herbicide removal from water using iron nano-composite material, Int. J. Environ. Sci. Technol., 13 (2016) 733–742.

[4] R. Nodehi, H. Shayesteh, A.R. Kelishami, Enhanced adsorption of congo red using cationic surfactant functionalized zeolite particles, Microchem. J., 153 (2020) 104281, doi: 10.1016/j.microc.2019.104281.

[5] V. Kumar, P. Saharan, A.K. Sharma, A. Umar, I. Kaushal, A. Mittal, Y. Al-Hadeethi, B. Rashad, Silver doped manganese oxide-carbon nanotube nanocomposite for enhanced dye-sequestration: isotherm studies and RSM modelling approach, Ceram. Int., 46 (2020) 10309–10319.

[6] J. Mittal, R. Ahmad, M.O. Ejaz, A. Mariyam, A. Mittal, A novel, eco-friendly bio-nanocomposite (Alg-Cst/Kal) for the adsorptive removal of crystal violet dye from its aqueous solutions, Int. J. Phytorem., 24 (2022) 796–807.

[7] Y. Majedi, E. Alhilali, M. Al Nehayan, A. Rashed, S.S. Ali, N. Al Rawashdeh, T. Thiemann, A. Soliman, Treatment of Dye-Loaded Wastewater With Activated Carbon From Date Palm Leaf Wastes, The 4th World Sustainability Forum, Canada, 2014, pp. 1–12.

[8] M. Hassaan, Advanced Oxidation Processes of Some Organic Pollutants in Fresh and Seawater, Ph.D., A Thesis, Faculty of Science, Port Said Univ., 2016.

[9] J. Mittal, A. Mariyam, F. Sakina, R.T. Baker, A.K. Sharma, A. Mittal, Batch and bulk adsorptive removal of anionic dye using metal/halide-free ordered mesoporous carbon as adsorbent, J. Cleaner Prod., 321 (2021) 129060, doi: 10.1016/j.jclepro.2021.129060.

[10] M.I. Khan, A. Shanableh, N. Nasir, S. Shahida, Adsorptive removal of methyl orange from wastewaters by the commercial anion exchange membrane EPTAC, Desal. Water Treat., 234 (2021) 245–254.

[11] M.I. Khan, N. Elboughdiri, A. Shanableh, M.H. Lashari, S. Shahida, Application of the commercial anion exchange membrane for adsorptive removal of Eriochrome Black-T from aqueous solution, Desal. Water Treat., 252 (2022) 437–448.

[12] M.I. Khan, A. Shanableh, J. Fernandez, M.H. Lashari, S. Shahida, S. Manzoor, S. Zafar, A. ur Rehman, N. Elboughdiri, Synthesis of DMEA-grafted anion exchange membrane for adsorptive discharge of methyl orange from wastewaters, Membranes, 11 (2021) 166, doi: 10.3390/membranes11030166.

[13] A.A. Oyekanmi, A. Ahmad, K. Hossain, M. Rafatullah, Statistical optimization for adsorption of Rhodamine B dye from aqueous solutions, J. Mol. Liq., 281 (2019) 48–58.

[14] A. Mariyam, J. Mittal, F. Sakina, R.T. Baker, A.K. Sharma, A. Mittal, Efficient batch and fixed-bed sequestration of a basic dye using a novel variant of ordered mesoporous carbon as adsorbent, Arabian J. Chem., 14 (2021) 103186, doi: 10.1016/j.arabjc.2021.103186.

[15] P. Saharan, V. Kumar, J. Mittal, V. Sharma, A.K. Sharma, Efficient ultrasonic assisted adsorption of organic pollutants employing bimetallic-carbon nanocomposites, Sep. Sci. Technol., 56 (2021) 2895–2908.

[16] R. Ahmad, I. Hassan, A. Mittal, Adsorption of Cr(VI) and Cd(II) on chitosan grafted polyaniline-OMMT nanocomposite: isotherms, kinetics and thermodynamics studies, Desal. Water Treat., 58 (2017) 144–153.

[17] A. Mariyam, J. Mittal, F. Sakina, R.T. Baker, A.K. Sharma, Adsorption behaviour of Chrysoidine R dye on a metal/halide-free variant of ordered mesoporous carbon, Desal. Water Treat., 223 (2021) 425–433.

[18] N.K. Mondal, S. Kar, Potentiality of banana peel for removal of Congo red dye from aqueous solution: isotherm, kinetics and thermodynamics studies, Appl. Water Sci., 8 (2018) 1–12.

[19] A. El-Maghraby, H. El Deeb, Removal of a basic dye from aqueous solution by adsorption using rice hulls, Global Nest J., 13 (2011) 90–98.

[20] M.I. Khan, S. Zafar, M.A. Khan, F. Mumtaz, P. Prapamonthon, A.R. Buzdar, *Bougainvillea glabra* leaves for adsorption of congo red from wastewater, Fresenius Environ. Bull., 27 (2018) 1456–1465.

[21] M.I. Khan, S. Zafar, A.R. Buzdar, M.F. Azhar, W. Hassan, A. Aziz, Use of citrus sinensis leaves as a bioadsorbent for removal of congo red dye from aqueous solution, Fresenius Environ. Bull., 27 (2018) 4679–4688.

[22] M.I. Khan, S. Zafar, M.F. Azhar, A.R. Buzdar, W. Hassan, A. Aziz, M. Khraisheh, Leaves powder of syzgium cumini as an adsorbent for removal of congo red dye from aqueous solution, Fresenius Environ. Bull., 27 (2018) 3342–3350.

[23] M.I. Khan, S. Zafar, H.B. Ahmad, M. Hussain, Z. Shafiq, Use of morus albal leaves as bioadsorbent for the removal of congo red dye, Fresenius Environ. Bull., 24 (2015) 2251–2258.

[24] H. Daraei, A. Mittal, Investigation of adsorption performance of activated carbon prepared from waste tire for the removal of methylene blue dye from wastewater, Desal. Water Treat., 90 (2017) 294–298.

[25] N.T.H. Nhung, B.T.P. Quynh, P.T.T. Thao, H.N. Bich, B.L. Giang, Pretreated Fruit Peels as Adsorbents for Removal of Dyes From Water, IOP Conf. Ser.: Earth Environ. Sci., 2018, doi: 10.1088/1755-1315/159/1/012015.

[26] H. Tahir, M. Sultan, N. Akhtar, U. Hameed, T. Abid, Application of natural and modified sugar cane bagasse for the removal of dye from aqueous solution, J. Saudi Chem. Soc., 20 (2016) S115–S121.

[27] M. Akl, M.B. Dawy, A.A. Serage, Efficient removal of phenol from water samples using sugarcane bagasse based activated carbon, J. Anal. Bioanal. Techol., 5 (2014) 1–12.

[28] L. Canilha, A.K. Chandel, T. Suzane dos Santos Milessi, F.A.F. Antunes, W. Luiz da Costa Freitas, M. das Graças Almeida Felipe, S.S. da Silva, Bioconversion of sugarcane biomass into ethanol: an overview about composition, pretreatment methods, detoxification of hydrolysates, enzymatic saccharification, and ethanol fermentation, J. Biomed. Biotechnol., 2012 (2012) 989572, doi: 10.1155/2012/989572.

[29] Y. Zhou, S. Yao, Y. Ma, G. Li, Q. Huo, Y. Liu, An anionic single-walled metal–organic nanotube with an armchair (3,3) topology as an extremely smart adsorbent for the effective and selective adsorption of cationic carcinogenic dyes, Chem. Commun., 54 (2018) 3006–3009.

[30] H. Masood, S. Zafar, H. Rehman, M.I. Khan, H.B. Ahmad, A. Naz, W. Hassan, M.H. Lashari, Adsorptive removal of anionic dyes in aqueous binary mixture by anion exchange membrane, Desal. Water Treat., 194 (2020) 248–258.

[31] F. Hanif, S. Ehsan, S. Zafar, M. Akhtar, M.I. Khan, M.F. Warsi, S. Mubarik, W. Hassan, I. Shakir, S. Manzoor, Adsorptive removal of methyl orange and acid blue-2445 from binary system by anion exchange membrane BI: non-linear and linear form of isotherms, Desal. Water Treat., 194 (2020) 290–301.

[32] S. Zafar, M.I. Khan, M. Khraisheh, M.H. Lashari, S. Shahida, M.F. Azhar, P. Prapamonthon, M.L. Mirza, N. Khalid, Kinetic, equilibrium and thermodynamic studies for adsorption of nickel ions onto husk of *Oryza sativa*, Desal. Water Treat., 167 (2019) 277–290.

[33] S. Zafar, M.I. Khan, M. Khraisheh, S. Shahida, T. Javed, M.L. Mirza, N. Khalid, Use of rice husk as an efective sorbent for the removal of cerium ions from aqueous solution: kinetic, equilibrium and thermodynamic studies, Desal. Water Treat., 150 (2019) 124–135.

[34] M.I. Khan, T.M. Ansari, S. Zafar, A.R. Buzdar, M.A. Khan, F. Mumtaz, P. Prapamonthon, M. Akhtar, Acid green-25 removal from wastewater by anion exchange membrane: adsorption kinetic and thermodynamic studies, Membr. Water Treat., 9 (2018) 79–85.

[35] M.I. Khan, S. Zafar, M.A. Khan, A.R. Buzdar, P. Prapamonthon, Adsorption kinetic, equilibrium and thermodynamic study for the removal of Congo red from aqueous solution, Desal. Water Treat., 98 (2017) 294–305.

[36] M.I. Khan, L. Wu, A.N. Mondal, Z. Yao, L. Ge, T. Xu, Adsorption of methyl orange from aqueous solution on anion exchange membranes: adsorption kinetics and equilibrium, Membr. Water Treat., 7 (2016) 23–38.

[37] M.I. Khan, S. Akhtar, S. Zafar, A. Shaheen, M.A. Khan, R. Luque, Removal of congo red from aqueous solution by anion exchange membrane (EBTAC): adsorption kinetics and themodynamics, Materials, 8 (2015) 4147–4161.

[38] R. Gao, X. Shen, L. Wang, Adsorption of basic magenta on graphene oxide-modified sugarcane bagasse, BioResources, 14 (2019) 8100–8113.

[39] M.I. Khan, J. Su, L. Guo, Development of high performance anion exchange membranes for diffusion dialysis process, Desal. Water Treat., 221 (2021) 281–290.

[40] M.I. Khan, J. Fernandez-Garcia, Q.-L. Zhu, Fabrication of doubly charged anion-exchange membranes for enhancing hydroxide conductivity, Sep. Sci. Technol., 56 (2020) 1589–1600.

[41] M.I. Khan, C. Zheng, A.N. Mondal, M.M. Hossain, B. Wu, K. Emmanuel, L. Wu, T. Xu, Preparation of anion exchange membranes from BPPO and dimethylethanolamine for electrodialysis, Desalination, 402 (2017) 10–18.

[42] N.R. Molaudzi, A.A. Ambushe, Sugarcane bagasse and orange peels as low-cost biosorbents for the removal of lead ions from contaminated water samples, Water, 14 (2022) 3395, doi: 10.3390/w14213395.

[43] S. Arif, S. Zafar, M. Imran Khan, S. Manzoor, A. Shanableh, J. Fernandez Garcia, M. Hayat, Removal of chromium(VI) by commercial anion exchange membrane BII from an aqueous solution: adsorption kinetic, equilibrium and thermodynamic studies, Inorg. Chem. Commun., 152 (2023) 110696, doi: 10.1016/j.inoche.2023.110696.

[44] I.W. Almanassra, M.I. Khan, A. Chatla, M. Ali Atieh, A. Shanableh, Utilization of palm leaves as an extraordinary adsorbent for the removal of Pb(II) from an aqueous solution, Desal. Water Treat., 271 (2022) 206–219.

[45] I.W. Almanassra, M.I. Khan, M.A. Atieh, A. Shanableh, Adsorption of lead ions from an aqueous solution onto

NaOH-modified rice husk, Desal. Water Treat., 262 (2022) 152–167.
[46] M.I. Khan, A. Shanableh, A.M. Alfantazi, M.H. Lashari, S. Manzoor, R. Anwer, N. Farooq, F.A. Harraz, M. Alsaiari, M. Faisal, Application of QPPO/PVA based commercial anion exchange membrane as an outstanding adsorbent for the removal of Eosin-B dye from wastewaters, Chemosphere, 321 (2023) 138006, doi: 10.1016/j.chemosphere.2023.138006.
[47] M.I. Khan, A. Shanableh, S. Manzoor, A. Rehman, S. Shahida, F. Ahmad, Application of United Arab Emirates *Arecaceae* leaves biochar for adsorptive removal of Rhodamine B from an aqueous solution, Desal. Water Treat., 283 (2023) 247–258.
[48] K. Parveen, S. Zafar, M.I. Khan, R. Anwer, A. Shanableh, Removal of eosin yellow from wastewaters by the commercial anion exchange membrane BI, Desal. Water Treat., 287 (2023) 245–253.
[49] S. Zafar, M.I. Khan, M. Khraisheh, S. Shahida, N. Khalid, M.L. Mirza, Effective removal of lanthanum ions from aqueous solution using rice husk: impact of experimental variables, Desal. Water Treat., 132 (2019) 263–273.
[50] S. Zafar, M.I. Khan, A. Shanableh, S. Ahmad, S. Manzoor, S. Shahida, P. Prapamonthon, S. Mubeen, A. Rehman, Adsorption of silver, thorium and nickel ions from aqueous solution onto rice husk, Desal. Water Treat., 236 (2021) 108–122.
[51] S. Zafar, M.I. Khan, N. Elboughdiri, M.H. Lashari, A. Shanableh, S. Shahida, S. Manzoor, Adsorption performance of rice husk towards copper ions from wastewater, Desal. Water Treat., 258 (2022) 133–142.
[52] P. Praipipat, P. Ngamsurach, A. Sanghuayprai, Modification of sugarcane bagasse with iron(III) oxide-hydroxide to improve its adsorption property for removing lead(II) ions, Sci. Rep., 13 (2023) 1467, doi: 10.1038/s41598-023-28654-5.
[53] M.A.K.M. Hanafiah, W.S.W. Ngah, S.H. Zolkafly, L.C. Teong, Z.A.A. Majid, Acid Blue 25 adsorption on base treated *Shorea dasyphylla* sawdust: kinetic, isotherm, thermodynamic and spectroscopic analysis, J. Environ. Sci., 24 (2012) 261–268.
[54] M. Ghanei, A. Rashidi, H.-A. Tayebi, M.E. Yazdanshenas, Removal of Acid Blue 25 from aqueous media by magnetic-SBA-15/CPAA super adsorbent: adsorption isotherm, kinetic, and thermodynamic studies, J. Chem. Eng. Data, 63 (2018) 3592–3605.
[55] F. Darvishalipour, H. Ghafouri Taleghani, M. Ghorbani, H. Salimi Kenari, Fabrication of nanoporous functionalized hydroxyapatite as high performance adsorbent for Acid Blue 25 dye removal, Int. J. Eng., 42 (2019) 193–200.
[56] S. Largergren, Zur theorie der sogenannten adsorption geloster stoffe, Kungliga Svenska Vetenskapsakademiens, Handlingar, 24 (1898) 1–39.
[57] M.I. Khan, M.H. Lashari, M. Khraisheh, S. Shahida, S. Zafar, P. Prapamonthon, A. Rehman, S. Anjum, N. Akhtar, F. Hanif, Adsorption kinetic, equilibrium and thermodynamic studies of Eosin-B onto anion exchange membrane, Desal. Water Treat., 155 (2019) 84–93.
[58] Y.-S. Ho, Second-order kinetic model for the sorption of cadmium onto tree fern: a comparison of linear and non-linear methods, Water Res., 40 (2006) 119–125.
[59] S. Zafar, M.I. Khan, M.H. Lashari, M. Khraisheh, F. Almomani, M.L. Mirza, N. Khalid, Removal of copper ions from aqueous solution using NaOH-treated rice husk, Emergent Mater., 3 (2020) 857–870.
[60] S. Zafar, N. Khalid, M. Daud, M.L. Mirza, Kinetic studies of the adsorption of thorium ions onto rice husk from aqueous media: linear and non-linear approach, The Nucleus, 52 (2015) 14–19.
[61] S. Zafar, M.I. Khan, M. Khraisheh, S. Shahida, N. Khalid, M.L. Mirza, Effective removal of lanthanum ions from aqueous solution using rice husk: impact of experimental variables, Desal. Water Treat., 132 (2018) 263–273.
[62] S. Zafar, M.I. Khan, H. Rehman, J. Fernandez-Garcia, S. Shahida, P. Prapamonthon, M. Khraisheh, A. Rehman, H.B. Ahmad, M.L. Mirza, N. Khalid, M.H. Lashari, Kinetic, equilibrium, and thermodynamic studies for adsorptive removal of cobalt ions by rice husk from aqueous solution, Desal. Water Treat., 204 (2020) 285–296.
[63] S. Zafar, M.I. Khan, W. Hassan, S. Mubeen, T. Javed, S. Shahida, S. Manzoor, A. Shanableh, M.L. Mirza, A. Rehman, N. Khalid, M.H. Lashari, Application of NaOH-treated rice husk for adsorptive discharge of cobalt ions from wastewater, Desal. Water Treat., 226 (2021) 328–338.